INSTITUTE OF PHYSICS PUBLISHING JOURNAL OF PHYSICS B: ATOMIC, MOLECULAR AND OPTICAL PHYSICS

J. Phys. B: At. Mol. Opt. Phys. **38** (2005) 4123–4134 doi:10.1088/0953-4075/38/22/015

Electron scattering from magnesium at an incident energy of 20 eV

D O Brown[1], A Crowe[1], D V Fursa[2], I Bray[2] and K Bartschat[3]

[1] School of Natural Sciences (Physics), University of Newcastle, Newcastle upon Tyne NE1 7RU, UK
[2] Centre for Atomic, Molecular and Surface Physics, Murdoch University, Perth, Australia
[3] Department of Physics and Astronomy, Drake University, Des Moines, IA 50311, USA

Received 16 June 2005, in final form 28 September 2005
Published 2 November 2005
Online at stacks.iop.org/JPhysB/38/4123

Abstract

Excitation of the $3\,^1$P state of magnesium by 20 eV electrons has been studied experimentally using the scattered-electron–polarized-photon correlation method over a wide range of scattering angles (10°–120°) and theoretically using the convergent close-coupling and *R*-matrix with pseudo-states methods. The measured linear Stokes parameters, and the circular polarization calculated from these parameters, assuming coherent excitation, are generally well produced by these theoretical models as well as by some previous theories. Relative differential cross sections for elastic scattering and excitation of the $3\,^1$P and $3\,^3$P states were also measured over the angular range 10°–140°. The results are compared with those from previous experiments and with present and previous theoretical predictions.

(Some figures in this article are in colour only in the electronic version)

1. Introduction

During the last decade, new theoretical methods have proved extremely reliable in predicting the detailed results of quantum mechanically complete correlation experiments for electron excitation of hydrogen, other quasi-one-electron atoms and helium. The convergent close-coupling (CCC) (Bray and Stelbovics 1992, Fursa and Bray 1997) and *R*-matrix with pseudo-states (RMPS) (Bartschat *et al* 1996a, 1996b) methods have been highly successful for a wide range of kinematics from near-threshold to high incident energies and over a wide range of scattering angles. For helium, this has included excitation of states with different angular momenta (Cvejanović and Crowe 1997) and multiplicity (Fursa *et al* 1997).

In order to test and help develop the CCC, RPMS and other theoretical approaches for heavier and more complex targets, we have extended our experimental studies to the quasi-two-electron atoms. In a recent paper (Brown *et al* 2003), we reported scattered-electron–polarized-photon correlations for the $3\,^1$P state of magnesium at an incident electron energy

of 40 eV and scattering angles up to 120°. The linear polarizations from that study were well reproduced by both the CCC (Fursa and Bray 2001) and RMPS methods. The relativistic distorted-wave (RDW) method of Kaur *et al* (1997) and the first-order many-body theory (FOMBT) of Meneses *et al* (1990) also showed substantial agreement with experiment. It might be expected that distorted-wave methods would work well at this energy of almost ten times the excitation threshold. There is also evidence that distorted-wave models perform better for heavier systems at low energies than for lighter targets such as helium. An example is the good agreement between the distorted-wave Born calculations of Bartschat and Madison (1987) and the angular correlation data of Gough and Crowe (1994) for the $[4p^5(^2P_{3/2})5s]^3P_1$ state of krypton at an incident energy within 5 eV of the excitation threshold.

In the present study, we test the latest close-coupling calculations at this energy and we also investigate whether the available distorted-wave calculations provide a reasonable description at a lower energy for a target with intermediate nuclear charge between helium and krypton. Specifically, we present the results of experimental studies using the scattered-electron–polarized-photon coincidence method for the $(3s^2)^1S \rightarrow (3s3p)^1P$ excitation process in magnesium by 20 eV incident electrons and the corresponding results of newly performed RMPS and CCC calculations. The measured differential Stokes parameters between 10° and 120° are transformed into the relevant charge-cloud (Andersen) parameters and compared with theory.

We have also measured relative differential cross sections (DCS) for elastic scattering and excitation of the $3\,^1P$ and $3\,^3P$ states, again at 20 eV incident energy. The results are compared with those from earlier experiments and with present and previous theoretical predictions.

2. Experimental apparatus and method

The apparatus has recently been described in detail by Brown *et al* (2003). Briefly, a beam of electrons crosses a beam of magnesium atoms from an oven operated at a maximum temperature of 723 K. Scattered electrons are focused into a hemispherical electrostatic analyser and those corresponding to a particular scattering process are transmitted and detected using a channel electron multiplier. The relative differential cross sections reported here are obtained from the angular distributions of scattered electrons with an energy loss corresponding to the excitation energy of the state being studied.

For the scattered-electron–polarized-photon correlation studies, the photons from the decay of the $(3s3p)^1P$ state are analysed and detected perpendicular ($+z$ direction) to the x–y scattering plane defined by the momenta of the incident and scattered electrons. In order to observe only photons from identically prepared states, an experimental condition necessary for coherent excitation, they are observed in coincidence with scattered electrons of a well-defined momentum. Specifically, the angle-differential Stokes parameters, P_1, P_2 and P_3, are measured, where

$$P_1 = \frac{I_z(0^\circ) - I_z(90^\circ)}{I_z(0^\circ) + I_z(90^\circ)}, \tag{2.1}$$

$$P_2 = \frac{I_z(45^\circ) - I_z(135^\circ)}{I_z(45^\circ) + I_z(135^\circ)} \tag{2.2}$$

and

$$P_3 = \frac{I\,(\mathrm{RHC}) - I\,(\mathrm{LHC})}{I\,(\mathrm{RHC}) + I\,(\mathrm{LHC})}. \tag{2.3}$$

For the linear polarizations, P_1 and P_2, $I_z(\alpha)$ are the electron–photon coincidence signals measured with the polarizer axis set at an angle α relative to the incident electron beam, for

some scattered electron angle θ. For the circular polarization, P_3, I (RHC) and I (LHC) refer to the intensities of right-handed and left-handed circularly polarized photons, respectively, again observed in coincidence with the scattered electrons. A small positional dependence of the photomultiplier tube (PMT) cathodic efficiency due to linear polarization was eliminated using a quarter-wave plate placed in front of the PMT window and behind the analysing optics. The measured polarizations $P_{\rm m}$ were also corrected for polarizer extinction ratio, optical acceptance angle (0.25 rad maximum) and electron beam divergence angle (0.01 rad), using the relationship (Ehlers and Gallagher 1973)

$$P_{\rm m} = \left[\frac{k_\parallel - k_\perp}{k_\parallel + k_\perp}\right]\left[\frac{1-\varepsilon}{1-\varepsilon P}\right]\left[\frac{1-3\zeta}{1-\zeta P}\right]P. \tag{2.4}$$

Here $k_\parallel$ and $k_\perp$ are the polarizer transmittances for the electric vectors parallel to and orthogonal to the polarizer axis, respectively. Furthermore, $\varepsilon = \psi^2/4$ and $\zeta = \xi^2/4$, where ψ is the optical acceptance angle and ξ is the electron beam divergence angle, both measured in radians.

The results are also expressed using parameters describing the shape and dynamics of the excited-state charge cloud (Andersen *et al* 1988, Andersen and Bartschat 2001). For S $\rightarrow$ P coherent excitation, these are readily expressed in terms of the measured Stokes parameters. The shape of the charge cloud, described by the relative width to length ratio, P_ℓ, and the charge-cloud alignment angle, γ, relative to the incident electron beam direction, are both determined from the linear polarizations P_1 and P_2 according to

$$P_\ell = \sqrt{P_1^2 + P_2^2}, \tag{2.5}$$

$$\gamma = 0.5\arg(P_1 + {\rm i}P_2). \tag{2.6}$$

The expectation value of the angular momentum transfer in the collision, perpendicular to the scattering plane, $L_\perp$, is given by the sign-reversed value of P_3,

$$L_\perp \equiv -P_3. \tag{2.7}$$

The total polarization is defined as

$$|P| = \sqrt{P_1^2 + P_2^2 + P_3^2} \tag{2.8}$$

and, therefore,

$$|P| = \sqrt{P_\ell^2 + P_3^2}. \tag{2.9}$$

The latter observable is especially useful when the excitation can be assumed to be coherent, as for this transition. Then the value of $|P|$ is unity and the magnitude of P_3 or $L_\perp$ can already be determined from the linear polarization data according to

$$|P_3| = \sqrt{1 - P_\ell^2}. \tag{2.10}$$

In principle, however, independent measurements of all three Stokes parameters provide the potentially critical opportunity of experimental consistency checks (Andersen and Bartschat 2001).

3. Theoretical methods

We have used two different implementations of the close-coupling formalism, the CCC and RMPS methods, to perform a theoretical analysis of e–Mg collisions. Since both methods have been described in detail elsewhere, we only summarize the aspects that are particularly relevant to the present study.

3.1. The CCC calculations

Similar to our previous calculations of e–Mg scattering (Fursa and Bray 2001), we use a nonrelativistic formulation and describe magnesium as an atom with two active electrons above an inert Mg^{2+} $(1s^22s^22p^2)^1S$ core. One-electron and two-electron polarization potentials were used to model core-excitation effects with a polarizability $\alpha = 0.28\,a_0^3$ and a cut-off radius $r_0 = 1.3a_0$, where a_0 is the Bohr radius. A set of one-electron orbitals with orbital angular momentum $l \leqslant 3$ was obtained by diagonalizing the quasi-one-electron Mg^+ Hamiltonian in a basis of Laguerre (Sturmian) functions. The Laguerre basis exponential fall-offs were chosen the same, $\lambda = 2.02$, for all l and the basis sizes were chosen as $N_l = 25 - l$. The first eight $l = 0, 1, 2$ orbitals and the first seven $l = 3$ orbitals were used in standard two-electron configuration-interaction (CI) calculations. The set of all possible two-electron antisymmetric configurations of the form 3s*nl* and 3p*nl* were built, resulting in 210 configurations.

The collision calculations were performed using a momentum–space formulation of the close-coupling method (Fursa and Bray 1995). The set of coupled integral equations for the half-on-shell T-matrix (Lippmann–Schwinger equations) is formulated and solved by reducing it to a set of linear equations and adopting an appropriate integration quadrature rule. An important feature of such a solution is the non-uniqueness of the half-on-shell T-matrix (Norcross 1969, Stelbovics and Bransden 1989) although the on-shell T-matrix stays unique. This often leads to a loss of accuracy for the calculated T-matrix elements. In this work, we use a generalization of the technique previously implemented for quasi-one-electron atoms (Bray 1994) and helium in the frozen-core approximation (Fursa and Bray 1995) where the kernel of the T-matrix equation is modified with the aim to project out the non-unique solutions. This technique requires all target states generated in the CI calculations to be included in the subsequent scattering calculations. This can lead to a large calculation (210 coupled states in the present work). In comparison to our previous e–Mg calculations (Fursa and Bray 2001), we dropped the 3d*nl* configurations in the present work to reduce the size of the collision problem. The reduction in the accuracy of the Mg wavefunctions proved to be marginal.

3.2. The RMPS calculations

In this paper, we present results obtained with two R-matrix models. These, and others, were described in detail by Bartschat *et al* (2004). The first is a 9-state model (RM9), in which the lowest nine physical target states of Mg were included in the close-coupling plus correlation expansion of the total scattering wavefunction. This model was used, for example, by Bartschat and Sadeghpour (2003) and the calculations reported by Sullivan *et al* (2003). To generate these states, we started with the 1s, 2s, 2p and 3s orbitals given by Clementi and Roetti (1974) for neutral Mg and then constructed a 3p orbital by optimizing the energies of the $(3s3p)^3P^o$ and $(3s3p)^1P^o$ states. We then constructed configuration-averaged physical 4s, 4p and 3d orbitals and also included the $(3s4s)^{3,1}S$, $(3s4p)^{3,1}P^o$ and $(3s4p)^{3,1}D$ states in the close-coupling expansion. As in the CCC model, all states were represented by multi-configuration expansions, including the ground-state configuration and all possible one-electron and two-electron excitations above the inert Mg^{2+} core.

The principal extension of the RMPS model is the attempt to simulate the coupling to the higher lying states of the discrete target spectrum and, even more importantly, to the target continuum. In addition, we further improved the description of the target states of interest by generating short-range 4s, 4p and 3d orbitals by optimizing the energies of the physical states. Coupling to the continuum was achieved by supplementing the physical 3s and 3p orbitals and the above pseudo-orbitals by further Sturmian-type

Table 1. Experimental Stokes parameters and derived charge-cloud parameters for excitation of the $3\,^1$P state of magnesium at an electron impact energy of 20 eV. Also shown is $P_{3\mathrm{calc}}$, derived from the measured linear Stokes parameters, its sign assumed from the measured P_3.

θ (deg)	P_1	P_2	P_3	γ (deg)	P_ℓ	$P_{3\mathrm{calc}}$
10	-0.52 ± 0.05	-0.71 ± 0.03	-0.37 ± 0.03	-62.95 ± 0.88	0.88 ± 0.03	-0.48 ± 0.03
15	-0.56 ± 0.05	-0.45 ± 0.05	-0.65 ± 0.05	-70.63 ± 2.10	0.68 ± 0.05	-0.70 ± 0.06
20	-0.48 ± 0.05	-0.19 ± 0.06	-0.72 ± 0.05	-79.09 ± 3.03	0.52 ± 0.05	-0.86 ± 0.06
25	-0.04 ± 0.07	-0.30 ± 0.07	-0.54 ± 0.07	-48.59 ± 6.80	0.30 ± 0.07	-0.95 ± 0.08
30	0.27 ± 0.05	-0.56 ± 0.06	-0.25 ± 0.05	-32.24 ± 2.55	0.62 ± 0.06	-0.79 ± 0.07
35	0.23 ± 0.07	-0.89 ± 0.08	-0.32 ± 0.07	-37.88 ± 2.27	0.87 ± 0.08	-0.40 ± 0.09
40	0.36 ± 0.08	-0.90 ± 0.10	-0.31 ± 0.11	-34.20 ± 2.56	0.96 ± 0.10	-0.26 ± 0.11
50			-0.45 ± 0.11			
60	-0.53 ± 0.10	-0.45 ± 0.09	-0.49 ± 0.13	-69.68 ± 3.78	0.70 ± 0.09	-0.72 ± 0.11
80	-0.62 ± 0.10	0.70 ± 0.11	0.29 ± 0.18	65.77 ± 3.24	0.93 ± 0.11	0.36 ± 0.13
100	0.40 ± 0.10	0.17 ± 0.13	0.52 ± 0.12	11.60 ± 8.46	0.44 ± 0.11	0.90 ± 0.14
120	0.83 ± 0.13	-0.23 ± 0.11	0.15 ± 0.18	-7.64 ± 3.59	0.86 ± 0.13	0.51 ± 0.14

pseudo-orbitals $\bar{5}$s–$\bar{8}$s, $\bar{5}$p–$\bar{8}$p, $\bar{5}$d–$\bar{7}$d and $\bar{4}$f–$\bar{6}$f with an exponential drop-off exponent $\alpha = 0.82$. This exponent was chosen according to the well-tested RMPS procedure of placing one pseudo-state per angular momentum in the discrete spectrum and the remaining states in the continuum. A total of 54 states were kept in the close-coupling expansion, for the following symmetries (the number of states is given in parentheses): $^1\mathrm{S^e}(10)$, $^3\mathrm{S^e}(5)$, $^3\mathrm{P^e}(3)$, $^3\mathrm{P^o}(6)$, $^1\mathrm{P^o}(6)$, $^3\mathrm{D^e}(5)$, $^1\mathrm{D^e}(6)$, $^3\mathrm{D^o}(3)$, $^1\mathrm{D^o}(3)$, $^3\mathrm{F^e}(1)$, $^3\mathrm{F^o}(3)$, $^1\mathrm{F^o}(3)$.

The inner-region calculations were performed with the well-known set of Belfast R-matrix codes (Berrington *et al* 1995). The R-matrix radius was chosen as $40a_0$, 25 continuum orbitals per angular momentum of the projectile were used to generate the R-matrix basis functions and T-matrix elements for total orbital angular momenta up to $L = 15$ were calculated numerically using the program FARM of Burke and Noble (1995) for the asymptotic region. To ensure convergence of the partial-wave expansion, contributions from higher angular momenta were approximated via a geometric extrapolation procedure.

4. Results and discussion

4.1. The correlation parameters

The measured linear Stokes parameters (P_1, P_2), the charge-cloud parameters (P_ℓ, γ) and the measured and calculated (using equation (2.10)) circular polarizations (P_3 and $P_{3\mathrm{calc}}$) are given in table 1. These same parameters, together with the total degree of polarization $|P|$ and the present CCC, RMPS and RM9 predictions, are shown in figure 1 as a function of electron scattering angle. The results are compared with the previous experimental data of Brunger *et al* (1989) at small scattering angles and also with previous RDW and FOMBT predictions.

The general behaviour of both linear Stokes parameters is well produced by the CCC and RMPS calculations, and also by the previous RDW and FOMBT theories. There is also qualitative agreement between the present experiment and that of Brunger *et al* (1989) over their restricted common angular range of 10°–20°. For P_1, it is only in the angular range 60°–120° that experiment discriminates in favour of the CCC and RMPS predictions. Similarly, the P_2 data above 80° show greater differences between the various theories and between theory and experiment.

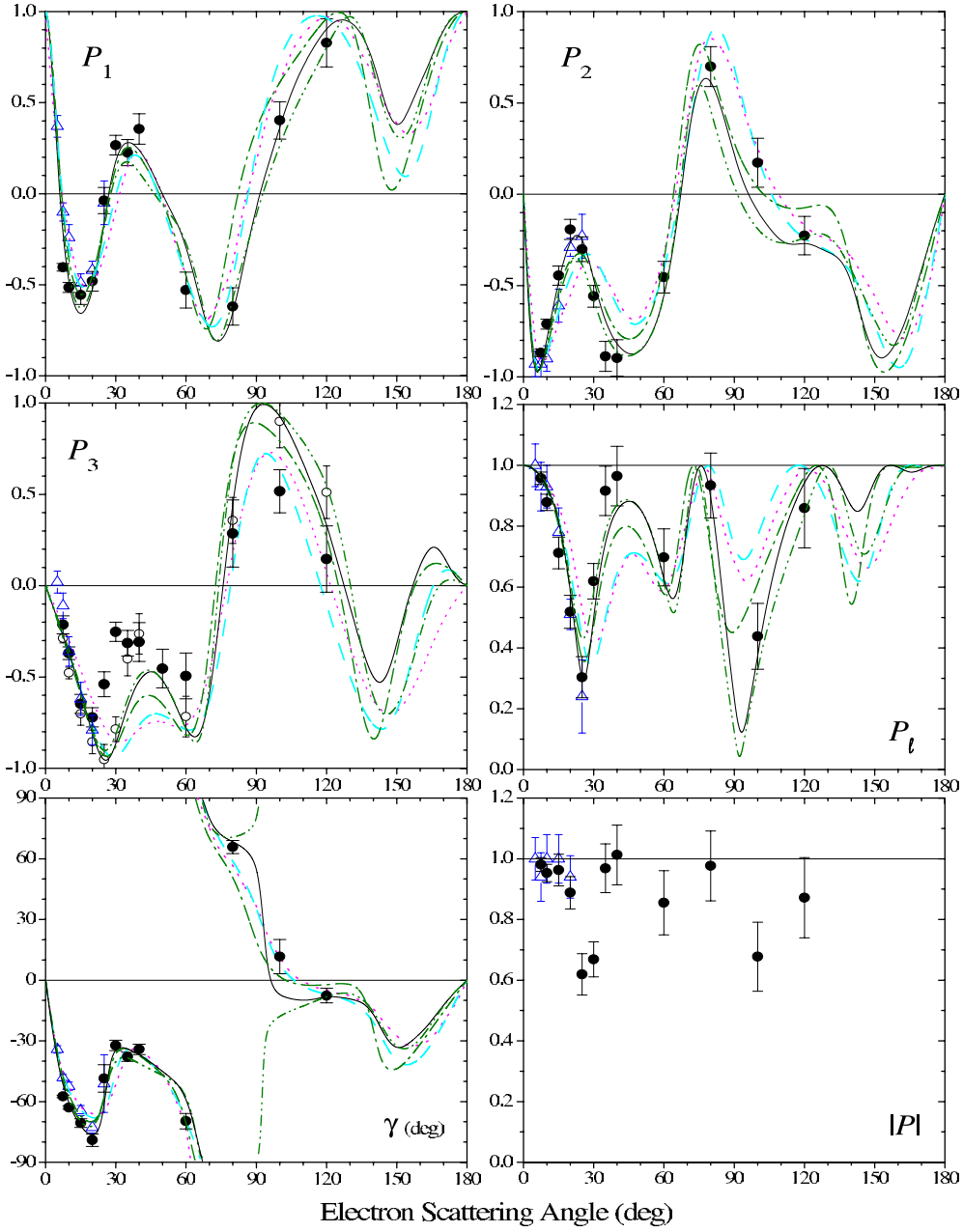

Figure 1. The Stokes and charge-cloud shape parameters, P_1, P_2, P_3, γ, P_ℓ, and the total polarization, P, for the $3\,^1$P state of magnesium at an incident electron energy of 20 eV as a function of electron scattering angle: (●) present measured data; (○) present P_3 data calculated from the measured P_1 and P_2 values and the sign chosen identical to the measured one; (△) Brunger *et al* (1989); (——) present CCC; (— · · —) present RMPS; (— · —) present RM9; (– – – – – –) RDW (Kaur *et al* 1997); (· · · · · ·) FOMBT (Meneses *et al* 1990).

The parameters P_ℓ and γ, derived from P_1 and P_2, that describe the shape of the charge cloud, exhibit complex and rapid variations with scattering angle. For P_ℓ, CCC and RMPS

show best agreement with experiment. However, this parameter emphasizes considerable differences with the other theories, RM9, RDW and FOMBT. These differences are particularly marked for the maximum close to 40° and the minimum close to 90°. In the case of γ, it is the RMPS calculation which differs most from the other calculations around a scattering angle of 90°. Note, however, that the values of γ in this angular range are highly sensitive to the way both P_1 and P_2 change sign. Physically, this can be easily understood since in the limit $P_1 = P_2 = 0$, a circular state is excited and γ is undefined, equation (2.6). Close to this condition, γ exaggerates very small differences in the near-zero values of P_1 and P_2 and the experimental uncertainty in γ also becomes large. Compared with the situation at 40 eV (Brown *et al* 2003), the P_2 parameter exhibits a similar angular behaviour. However, the large negative values of P_1 around 70° are not seen at 40 eV.

The variation of $P_3 \equiv -L_\perp$ again shows qualitative agreement between experiment and all theoretical predictions. As the scattering angle increases, P_3 initially drops to almost -1, corresponding to a nearly circular state. Well-defined structure in the range 20°–65° is followed by a positive peak around 95°. There is quantitative agreement between the present CCC and RMPS calculations while the two distorted-wave data sets differ substantially from them, especially near the minimum in the negative values around 45°. The RM9 results lie between these two sets. This is consistent with the fact that the RM9 contains more channel coupling than the distorted-wave models, but less than CCC and RMPS.

Quantitatively, there are major discrepancies between the measured and theoretical P_3 over the experimental angular range. The experimental magnitudes of the negative values at 25°, 30°, 35° and 40° are significantly smaller than predicted by the theories. This is of concern experimentally because of their inconsistency with the values of $P_{3\mathrm{calc}}$ calculated from the linear polarization data using equation (2.10). A similar observation was made at 40 eV by Brown *et al* (2003). Exhaustive experimental checks and a discussion of physical effects which could lead to reduced magnitudes of directly measured P_3 were reported in detail in that paper. The values of $P_{3\mathrm{calc}}$ obtained from the measured linear polarizations P_1 and P_2 agree with theory at 25° and 30° but still show a discrepancy with CCC and RMPS at 35° and 40°.

These small measured negative values of P_3 lead to values of $|P|$ less than unity in this angular range when the three Stokes parameters are combined using equation (2.8). This result seems difficult to physically justify for an S → P transition in a relatively light atom, and it is inconsistent with currently accepted theory.

4.2. Differential cross sections

The angular distributions of outgoing electrons following elastic scattering and excitation of the $3\,^1$P and $3\,^3$P states have been measured at an incident electron energy of 20 eV, the $3\,^1$P measurement as a routine preliminary to the coincidence measurements. For ease of comparison with theoretical predictions and previous experimental data, the DCS results are presented on an absolute differential cross-section scale by normalizing each to present theory so as to give a best overall visual fit in each case. All three DCS results are shown in figure 2. Errors shown for the present data are statistical uncertainties (one standard deviation).

The present experimental results for elastic scattering show that the DCS drop by almost three orders of magnitude to a minimum at 55°. This is followed by a broad maximum around 80°–90° and a further minimum near 130°. This behaviour is in general agreement with the only previous experimental results of Williams and Trajmar (1978). Their absolute scale was derived from normalization to the absolute $3\,^1$P excitation function of Leep and Gallagher (1976). The present CCC and RMPS calculations are in excellent agreement with each other

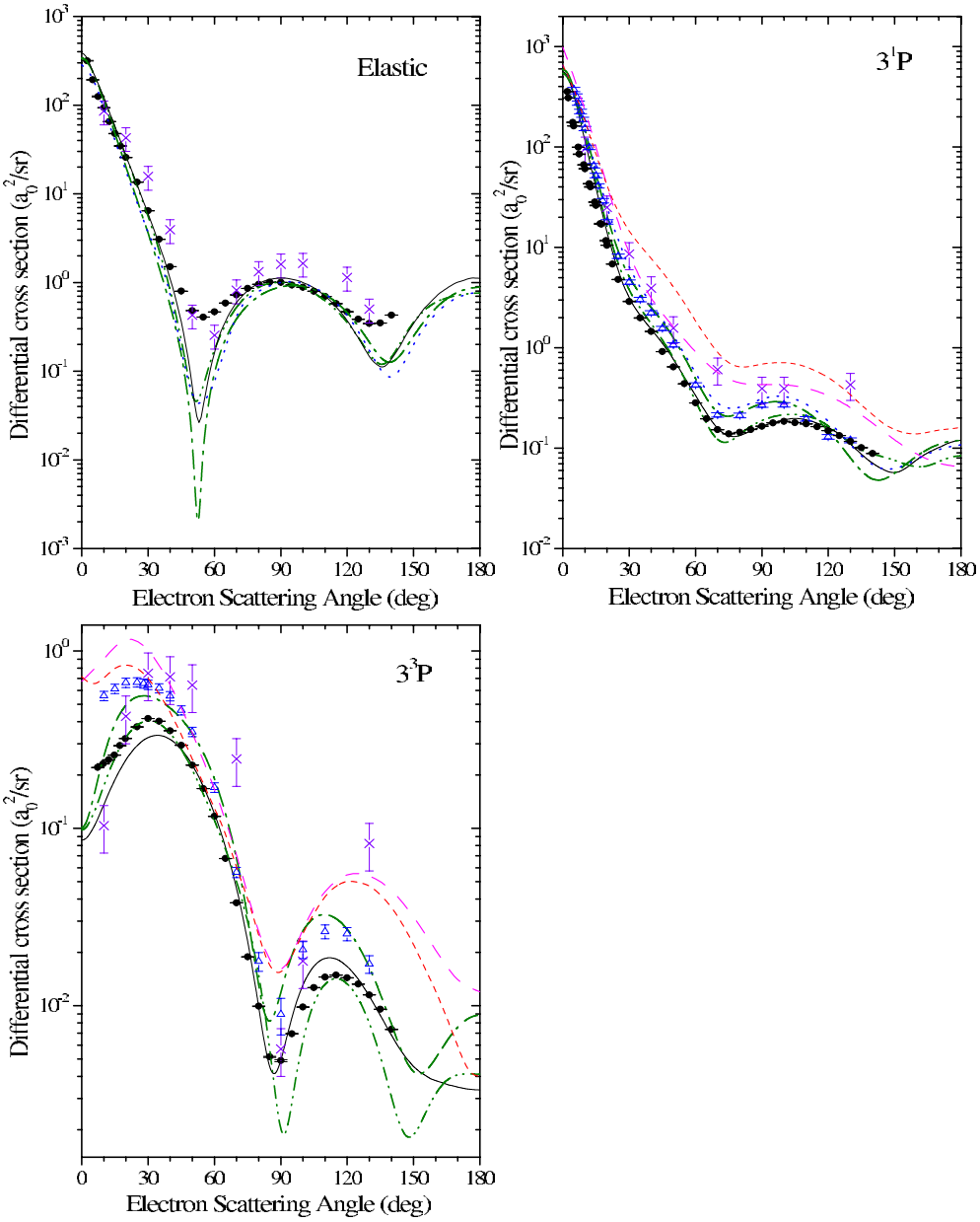

Figure 2. Differential cross sections for elastic scattering and excitation of the 3 ^{1}P and 3 ^{3}P states of magnesium at 20 eV: (●) present data; (△) Brunger *et al* (1989) (3 ^{1}P), Houghton *et al* (1994) (3^{3}P); (×) Williams and Trajmar (1978); (——) present CCC; (— · · —) present RMPS; (— · —) present RM9; (· · · · · ·) Mitroy and McCarthy (1989); (— — —) FOMBT (Meneses *et al* 1990); (- - - -) RDW (Kaur *et al* 1997).

while RM9 differs most in the region of the first minimum. Earlier five-state close-coupling predictions of Mitroy and McCarthy (1989) are also in good agreement with the present calculations. The principal difference between the present experiment and the theories is in

the depths of the two minima. As discussed by Brown *et al* (2003), the present experiment cannot quantify or isolate any contribution to elastic scattering from possible impurity species. Even a relatively small contribution to the signal from sources other than magnesium could lead to a filling of these minima without much distortion of the overall shape. The theoretical minima are not narrow enough for the discrepancy to be due to the experimental angular resolution.

The $3\,^1$P DCS falls to a minimum around 70° with a change in slope around 30°. A broad maximum is seen around 100°. The present experimental data exhibit the same general shape as the previous data of Brunger *et al* (1989) and of Williams and Trajmar (1978). The CCC and RMPS calculations agree best with the present experiment in shape and also with each other in magnitude. The RDW and FOMBT calculations yield substantially larger cross sections at higher angles.

Cross sections for optically allowed transitions are often put on an absolute scale using a generalized oscillator strength method (GOS) (Mott and Massey 1965). However, we have decided against that method here. Experimental concerns about the application of this normalization method have already been expressed by Brown *et al* (2003). In the present case of 20 eV incident energy, in particular, the measured angular dependence of the cross section at small scattering angles disagrees with theory. Note that these are the same small momentum transfer data used in GOS normalization. There are also theoretical concerns about this normalization method at lower energies, since the basis of the GOS approach is similar to that of the first Born approximation. The value of OOS = 1.723 calculated by Fursa and Bray (2001) is within 6% of the most recent experimental data of Kelly and Mathur (1980) and of Liljeby *et al* (1980). At 20 eV, the close-coupling methods give a GOS close to 1.0 at 0° and a GOS close to 1.2 if linearly extrapolated to zero momentum transfer, but yet this needs to be consistent with the OOS. This indicates the difficulty of normalizing experiment utilizing the forward angle data with extrapolation to zero momentum transfer. Very recently, it has been shown for ^{1}P excitation in zinc (Fursa *et al* 2005) that given reliable small angle data, the forward scattering function normalization method of Felfli *et al* (1998) can give cross sections to within about ≈10%.

The $3\,^3$P state DCS exhibits a very different shape and is about three orders of magnitude smaller compared to that for elastic scattering and the optically allowed $3\,^1$P excitation at 20 eV. The $3\,^3$P state cross section has a maximum value at 30° in contrast to the rapid fall from the forward direction for both elastic scattering and the $3\,^1$P state. The decrease in the DCS at small angles was predicted by previous experiments (Williams and Trajmar 1978, Houghton *et al* 1994) and by the FOMBT (Meneses *et al* 1990), RDW (Kaur *et al* 1997) and close-coupling (McCarthy *et al* 1989) calculations. If the present experimental data were normalized to give a good fit to the absolute data of Houghton *et al* (1994), they would show very good agreement, with the exception of a few points in the forward direction. Their data were put on an absolute scale by normalization to their $3\,^1$P cross sections (Brunger *et al* 1988). There is also reasonable agreement with the data of Williams and Trajmar (1978), except for the data at both extremes of their angular range. Although the present theories reproduce the same overall shape as experiment, there are substantial differences between them and no normalization of the present data brings experiment and theory into good agreement over the full measured angular range. The present normalization shows that the ratio between the two maxima is better reproduced by the RMPS model, while the width and position of the minimum around 90° are best reproduced by the CCC. As is typically the case for optically forbidden transitions, theories that do not include channel coupling at all (such as the distorted-wave models) or only coupling between a few physical states (like RM9) predict significantly bigger cross sections than CCC and RMPS.

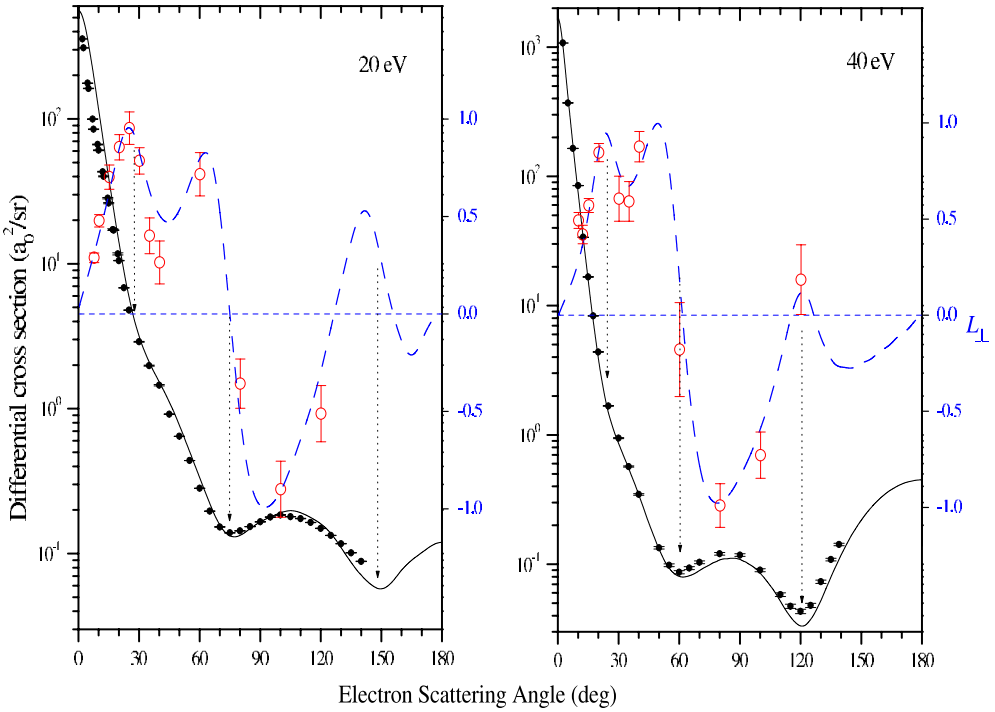

Figure 3. Differential cross sections and $L_\perp$ for excitation of the 3 ^{1}P state of magnesium: (○) $L_\perp$ calculated from experimental linear Stokes parameters, present data at 20 eV, Brown *et al* (2003) at 40 eV; (●) corresponding experimental DCS; (- - - -) $L_\perp$, present CCC at 20 eV, Fursa and Bray (2001) at 40 eV; (——) corresponding DCS.

In figure 3, attention is drawn to what appears to be a universal relationship between features in the DCS and the angular momentum transfer $L_\perp$. The present experimental data are shown for the 3 ^{1}P state at 20 eV and those of Brown *et al* (2003) at 40 eV. For clarity, only the present CCC calculation is shown at 20 eV and that of Fursa and Bray (2001) at 40 eV. The most obvious similarity in both cases is the common angular position of the first minimum in the DCS and the first zero value of $L_\perp$ at a non-zero scattering angle. This relationship was first observed by Teubner and Scholten (1992) for the 3 ^{2}P$_{3/2}$ state of sodium and then for the 4 ^{1}P state of calcium by Law and Teubner (1995). A review of available data for the n ^{1}P states of the alkaline earth atoms (Cvejanović *et al* 2005) shows the same effect for all of them.

The presence of maxima and minima in the DCS can be interpreted in terms of electron diffraction effects. A number of ideas have been put forward to describe the angular behaviour of $L_\perp$ with electron scattering angle. Recall that $L_\perp$ and the magnetic sublevel cross sections, σ_M, in the natural co-ordinate system, are related by (Andersen *et al* 1988, Andersen and Bartschat 2001)

$$L_\perp \sim \frac{\sigma_{+1} - \sigma_{-1}}{\sigma_{+1} + \sigma_{-1}}. \tag{4.1}$$

Hence, $L_\perp = 0$ requires $\sigma_{+1} = \sigma_{-1}$, and at a DCS minimum both cross sections are small. Unless there is a propensity for $\sigma_{+1} \approx \sigma_{-1}$ at DCS minima, this very simple approach is not helpful in understanding the relationship. It may be that the most physical explanation comes from an extension of the analysis presented by Madison *et al* (1986), who concluded that the

angular behaviour of $L_\perp$ is due to quantum mechanical interference between distorted partial waves.

At 40 eV, the near-zero $L_\perp$ around 120° corresponds with the second DCS minimum. At 20 eV, theory shows close, but not exact, agreement between the position of the third $L_\perp$ zero crossing and the second DCS minimum, but the negative to positive crossing does not appear to correspond to any feature in the DCS. At both energies, one can also point to similarities in the positions of the first maximum in $L_\perp$ and a change of slope in the DCS.

5. Conclusions

As previously observed at 40 eV, the excellent agreement between the measured linear Stokes parameters, P_1 and P_2, and the circular polarization, P_3, calculated from the measured linear polarizations assuming coherent excitation, and the CCC and RMPS predictions confirm the ability of these theories to describe the strong resonance excitation in magnesium. The RDW and FOMBT approaches also give substantial agreement with experiment. Relative differential cross sections for elastic scattering and excitation of the $3\,^1$P and $3\,^3$P states also provide a valuable test of available theories. For the present case of a relatively low incident electron energy of 20 eV, there is excellent agreement between experiment and CCC/RMPS for elastic scattering and very good agreement for all but the forward direction for the optically allowed $3^1\mathrm{S} \rightarrow 3^1\mathrm{P}$ transition. Some discrepancies, however, remain between theory and experiment for the forbidden $3^1\mathrm{S} \rightarrow 3^3\mathrm{P}$ transition.

Acknowledgments

EPSRC support is gratefully acknowledged. DOB acknowledges a studentship from the University of Newcastle. KB acknowledges support from the United States National Science Foundation through grant PHY-0244470. IB and DVF acknowledge support of the Australian Research Council and the Maui High Performance Computer Center.

References

Andersen N and Bartschat K 2001 *Polarization, Alignment, and Orientation in Atomic Collisions* (New York: Springer)
Andersen N, Gallagher J W and Hertel I V 1988 *Phys. Rep.* **165** 1–188
Bartschat K, Hudson E T, Scott M P, Burke P G and Burke V M 1996a *J. Phys. B: At. Mol. Opt. Phys.* **29** 115–23
Bartschat K, Hudson E T, Scott M P, Burke P G and Burke V M 1996b *J. Phys. B: At. Mol. Opt. Phys.* **29** 2875–85
Bartschat K and Madison D H 1987 *J. Phys. B: At. Mol. Phys.* **20** 5839–63
Bartschat K and Sadeghpour H R 2003 *J. Phys. B: At. Mol. Opt. Phys.* **36** L9–15
Bartschat K, Zatsarinny O, Bray I, Fursa D V and Stelbovics A T 2004 *J. Phys. B: At. Mol. Opt. Phys.* **37** 2617–39
Berrington K A, Eissner W N and Norrington P H 1995 *Comput. Phys. Commun.* **92** 290–420
Bray I 1994 *Phys. Rev.* A **49** 1066–82
Bray I and Stelbovics A T 1992 *Phys. Rev.* A **46** 6995–7011
Brown D O, Cvejanović D and Crowe A 2003 *J. Phys. B: At. Mol. Opt. Phys.* **36** 3411–23
Brunger M J, Riley J L, Scholten R E and Teubner P J O 1988 *J. Phys. B: At. Mol. Opt. Phys.* **21** 1639–48
Brunger M J, Riley J L, Scholten R E and Teubner P J O 1989 *J. Phys. B: At. Mol. Opt. Phys.* **22** 1431–42
Buckman S J, Noble C J and Teubner P J O 1979 *J. Phys. B: At. Mol. Phys.* **12** 3077–91
Burke V M and Noble C J 1995 *Comput. Phys. Commun.* **85** 471–500
Clementi E and Roetti C 1974 *At. Data Nucl. Data Tables* **14** 177
Cvejanović D and Crowe A 1997 *Phys. Rev. Lett.* **80** 3033–36
Cvejanović D, Crowe A and Brown D 2005 *Electron Scattering: From Atoms, Molecules, Nuclei and Bulk Matter* ed C T Whelan and N J Mason (New York: Kluwer Academic/Plenum) pp 23–32
Ehlers V J and Gallagher A 1973 *Phys. Rev.* A **7** 1573–85

Felfli Z, Msezane A Z and Bessis D 1998 *Phys. Rev. Lett.* **81** 963–6
Fursa D V and Bray I 1995 *Phys. Rev.* A **52** 1279–97
Fursa D V and Bray I 1997 *J. Phys. B: At. Mol. Opt. Phys.* **30** 757–85
Fursa D V and Bray I 2001 *Phys. Rev.* A **63** 032708
Fursa D, Bray I, Donnelly B P, McLaughlin D T and Crowe A 1997 *J. Phys. B: At. Mol. Opt. Phys.* **30** 3459–73
Fursa D V, Bray I, Panajotovic R, Sevic D, Pejcev V, Filipovic D M and Marinkovic 2005 *Phys. Rev.* A **72** 012706
Gough S F and Crowe A 1994 *J. Phys. B: At. Mol. Opt. Phys.* **27** 955–64
Houghton R K, Brunger M J, Shen G and Teubner P J O 1994 *J. Phys. B: At. Mol. Opt. Phys.* **27** 3573–80
Kaur S, Srivastava R, McEachran R P and Stauffer A D 1997 *J. Phys. B: At. Mol. Opt. Phys.* **30** 1027–42
Kelly F M and Mathur A D 1980 *Can. J. Phys.* **58** 1416–9
Law M R and Teubner P J O 1995 *J. Phys. B: At. Mol. Opt. Phys.* **28** 2257–67
Leep D and Gallagher A 1976 *Phys. Rev.* A **13** 148–55
Liljeby L, Lindgard A, Manervik S, Veje E and Jelemkovic B 1980 *Phys. Scr.* **21** 805–10
Madison D H, Csanak G and Cartwright D C 1986 *J. Phys. B: At. Mol. Phys.* **19** 3361–6
McCarthy I E, Ratnavelu K and Zhou Y 1989 *J. Phys. B: At. Mol. Opt. Phys.* **22** 2597–603
Meneses G D, Pagan C B and Machado L E 1990 *Phys. Rev.* A **41** 4740–50
Mitroy J and McCarthy I E 1989 *J. Phys. B: At. Mol. Opt. Phys.* **22** 641–5
Mott N F and Massey H S W 1965 *Theory of Atomic Collisions* (London: Oxford University Press)
Norcross D W 1969 *J. Phys. B: At. Mol. Phys.* **2** 1300–3
Stelbovics A T and Bransden B H 1989 *J. Phys. B: At. Mol. Opt. Phys.* **22** L451–4
Sullivan J P, Burrow P D, Newman D S, Bartschat K, Michejda J A, Panajotovic R, Moghbelalhossein M, McEachran R P and Buckman S J 2003 *New J. Phys.* **5** 159.1–26
Teubner P J O and Scholten R E 1992 *J. Phys. B: At. Mol. Opt. Phys.* **25** L301–6
Williams W and Trajmar S 1978 *J. Phys. B: At. Mol. Phys.* **11** 2021–29